The role of coherent vorticity in turbulent transport in resistive drift-wave turbulence

W. J. T. Bos,[1,2] S. Futatani,[3,4] S. Benkadda,[3] M. Farge,[5] and K. Schneider[1]
[1]*M2P2-CNRS & CMI, Université de Provence, 39, rue Joliot-Curie 13453 Marseille Cedex 13, France*
[2]*LMFA-UMR 5509-CNRS-Ecole Centrale de Lyon, Université Claude Bernard Lyon 1, INSA de Lyon, 69134 Ecully Cedex, France*
[3]*France-Japan Magnetic Fusion Laboratory LIA 336 CNRS/UMR 6633, CNRS-Université de Provence, Case 321, 13397 Marseille Cedex 20, France*
[4]*Graduate School of Energy Science, Kyoto University, Kyoto, Japan*
[5]*LMD-IPSL-CNRS, Ecole Normale Supérieure, 24 rue Lhomond, 75231 Paris Cedex 05, France*

(Received 7 March 2008; accepted 19 June 2008; published online 22 July 2008)

The coherent vortex extraction method, a wavelet technique for extracting coherent vortices out of turbulent flows, is applied to simulations of resistive drift-wave turbulence in magnetized plasma (Hasegawa–Wakatani system). The aim is to retain only the essential degrees of freedom, responsible for the transport. It is shown that the radial density flux is carried by these coherent modes. In the quasi-hydrodynamic regime, coherent vortices exhibit depletion of the polarization-drift nonlinearity and vorticity strongly dominates strain, in contrast to the quasi-adiabatic regime. © *2008 American Institute of Physics*. [DOI: 10.1063/1.2956640]

I. INTRODUCTION AND GOVERNING EQUATIONS

One important issue in fusion research is the understanding and control of turbulent radial flux of particles and heat in magnetized plasmas, in order to improve the confinement properties of fusion devices.[1] Indeed turbulence enhances the radial diffusion dramatically compared to neoclassical estimations. A long-standing question has been as follows:[2–6] what is the role of coherent structures in this radial transport? The answer to this question requires extracting and characterizing coherent structures. A particularly appropriate framework to identify coherent structures is the wavelet representation, where wavelets are basis functions well localized in both physical and Fourier space.[7] It has already been used to identify coherent structures in fluid turbulence and to distinguish them from background incoherent noise.[8] These methods have recently been applied to experimental signals of ion density in the tokamak scrape-off layer,[9] separating coherent bursts from incoherent noise. In the present work, these methods are applied to assess the role of coherent vorticity structures in anomalous radial transport in two-dimensional numerical simulations of drift-wave turbulence. Drift waves are now generally considered to play a key role in the dynamics and transport properties of tokamak edge turbulence (e.g., Ref. 10 and references therein). At the edge, the plasma temperature is low and the collision rate relatively large, therefore the resistivity is potentially important. The Hasegawa-Wakatani model[11,12] is a two-field model which includes the main features of turbulent transport by resistive drift waves.

In the present work, the two-dimensional slab geometry version of this model is chosen as a paradigm for drift-wave turbulence in the plasma-edge region. In dimensionless form, the Hasegawa–Wakatani model reads[13]

$$\left(\frac{\partial}{\partial t} - D\nabla^2\right)n + \kappa\frac{\partial\phi}{\partial y} + c(n-\phi) = [n,\phi], \tag{1}$$

$$\left(\frac{\partial}{\partial t} - \nu\nabla^2\right)\nabla^2\phi + c(n-\phi) = [\nabla^2\phi,\phi], \tag{2}$$

with n the plasma density fluctuation and ϕ the electrostatic potential fluctuation. D and ν are the cross-field diffusion of plasma density fluctuations and kinematic viscosity, respectively. The Poisson brackets are defined as

$$[a,b] = \frac{\partial a}{\partial x}\frac{\partial b}{\partial y} - \frac{\partial a}{\partial y}\frac{\partial b}{\partial x}. \tag{3}$$

We identify the x coordinate with the radial direction and the y coordinate with the poloidal direction. The equilibrium density n_0 is nonuniform, with a density gradient dn_0/dx in the negative x direction, such that the equilibrium density scale $L_n = n_0/(dn_0/dx)$ is constant and the value of κ is 1. The plasma density fluctuations n are normalized by n_0, therefore $n/n_0 \to n$, the electrostatic potential is normalized as $e\phi/T_e \to \phi$, the space as $x/\rho_s \to x$, and the time as $\omega_{ci}t \to t$, where e is the electron charge, T_e is the electron temperature, ω_{ci} is the ion cyclotron frequency, and $\rho_s = (m_i T_e)^{1/2}/(eB)$ is the ion integral length scale. B is the strength of the equilibrium magnetic field in the z direction and m_i is the ion mass. The key parameter in this model is the adiabaticity c, which represents the strength of the parallel electron resistivity. It is defined as

$$c = \frac{T_e k_\parallel^2}{e^2 n_0 \eta \omega_{ci}}, \tag{4}$$

with $k_\parallel$ the effective parallel wavenumber and η the electron resistivity.

The vorticity ω is related to the electrostatic potential ϕ by

$$\nabla^2\phi = \omega. \tag{5}$$

Note that for $c=0$, Eq. (1) corresponds to the advection-diffusion of a passive scalar in the presence of a (unity) mean

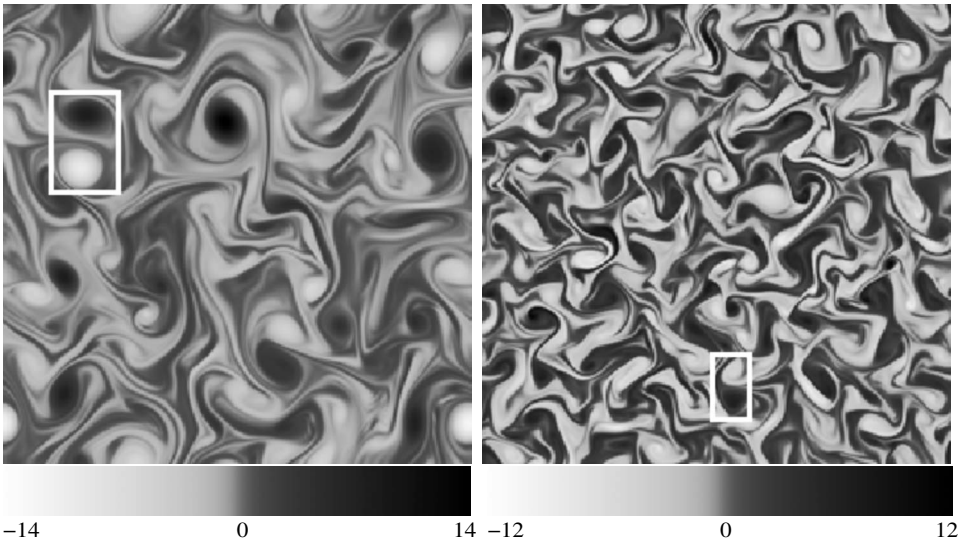

FIG. 1. One realization of the vorticity field for the quasi-hydrodynamic case (left) and for the quasi-adiabatic case (right). The abscissa corresponds to the radial position. The ordinate indicates the poloidal position. Both range from 0 to 64 ρ_s. The white frames indicate the dipoles we have selected in both cases.

scalar gradient in the x direction. Equation (2) corresponds in this case to the vorticity equation. For $c\to\infty$, the Hasegawa–Mima[14] one-field approximation is approached,[15] which ignores all resistive effects. For $c\to 0$, we recover the hydrodynamic limit, which is less relevant to describe edge fusion-plasma. Here two cases will be considered: a quasi-adiabatic case with $c=0.7$, and a quasi-hydrodynamic case with $c=0.01$. The case $c=0.7$ is generally considered to be the most relevant for tokamak-research and has been investigated in several other works (e.g., Refs. 4 and 15). Both cases differ from the fluid-dynamical case in that the velocity field is forced through the interaction term $c(n-\phi)$. The influence of this term on the density field can, however, be considered to be negligible in the quasi-hydrodynamic case.[6]

The quantity of interest, the radial particle density flux, is the correlation between the radial velocity $u_r=-\partial\phi/\partial y$ and the particle density,

$$\Gamma_r=\langle nu_r\rangle, \tag{6}$$

where the brackets denote an average over both time and space. The question we address in this paper is how coherent structures contribute to this flux. To investigate this, direct numerical simulations of the Hasegawa–Wakatani system are performed on a periodic domain discretized with $N=512^2$ grid points. The length of the domain is 64 ρ_s. A finite-difference method is used in which the nonlinear terms are computed using a method developed by Arakawa.[16] The time stepping is performed using a predictor-corrector scheme. The plasma density diffusion D and viscosity ν are set to 0.01 in normalized units. Computations are performed up to $t=612$. At $t\approx 100$, the kinetic energy saturates and a statistically stationary state is reached, independent of the (random) initial conditions. Typical realizations of the vorticity field are shown in Fig. 1, where one observes coherent structures for both cases. In each case, we select a dipolar structure that we indicate by a white frame. The quasi-hydrodynamic case exhibits coherent vortices of very different sizes and intensities, in contrast to the quasi-adiabatic case in which the coherent structures are more similar in size and intensity.

II. COHERENT VORTEX EXTRACTION (CVE)

A. Method

Definitions and details on the orthogonal wavelet transform and its extension to higher dimensions can be found, e.g., in Refs. 7 and 17. In the following, we fix the notation for the orthogonal wavelet decomposition of a two-dimensional scalar valued field. The wavelet transform unfolds the field into scales, positions, and directions using a set of dilated, translated, and rotated functions, called wavelets. Each wavelet is well-localized in space, oscillating (i.e., it has at least a vanishing mean, or better its first m moments vanish), and smooth (i.e., its Fourier transform exhibits fast decay for wavenumbers tending to infinity). We apply the coherent vortex extraction (CVE) algorithm[8,18] here using orthogonal wavelets. In dimension two, orthogonal wavelets span three directions (horizontal, vertical, and diagonal), due to the tensor product construction. To go from one scale to the next, wavelets are dilated by a factor 2 and the translation step doubles accordingly. Wavelet coefficients are thus represented on a dyadic grid.[7]

We apply the CVE algorithm to the vorticity fields ω of both the quasi-hydrodynamic and the quasi-adiabatic regime. The extraction is performed from the vorticity since enstrophy is an inviscid invariant in the hydrodynamic limit. Moreover, vorticity is Galilean invariant in contrast to velocity and streamfunction. We consider the quasistationary state of the simulations, i.e., when a saturated regime is reached, and we decompose the vorticity field, given at resolution $N=2^{2J}$, into an orthogonal wavelet series,

$$\omega(x,y)=\sum_{\lambda\in\Lambda}\tilde{\omega}_\lambda\psi_\lambda(x,y), \tag{7}$$

where the multi-index $\lambda=(j,i_x,i_y,d)$ denotes the scale j, the position $\boldsymbol{i}=(i_x,i_y)$, and the three directions $d=1,2,3$, corresponding to horizontal, vertical, and diagonal wavelets, respectively. The corresponding index set Λ is $\Lambda=\{\lambda=(j,i_x,i_y,d), j=0,\ldots,J-1; i_x,i_y=0\ldots 2^j-1, d=1,2,3\}$. Due to orthogonality, the wavelet coefficients are given by

TABLE I. Compression rate (% of coefficients retained), retained energy $E=\frac{1}{2}\langle\phi\nabla^2\phi\rangle$, enstrophy $Z=\frac{1}{2}\langle\omega^2\rangle$, and radial flux Γ_r, after applying the CVE filter to the vorticity field of the quasi-hydrodynamic and quasi-adiabatic 2D drift-wave turbulence simulations.

	Compr. (%)	E (%)	Z (%)	Γ_r (%)
Quasi-hydrodynamic ($c=0.01$)	1.3	99.9	97	99
Quasi-adiabatic ($c=0.7$)	1.8	99.0	93	98

$\tilde{\omega}_\lambda=\langle\omega,\psi_\lambda\rangle$, where $\langle\cdot,\cdot\rangle$ denotes the L^2-inner product defined as $\langle f,g\rangle=\int f(x,y)g(x,y)dxdy$. The wavelet coefficients measure fluctuations of ω at scale 2^{-j} around the position $\boldsymbol{i}$, in one of the three directions d. Here a Coifman 30 wavelet is used, which is orthogonal and has 10 vanishing moments[17] $[\int x^n\psi(x)dx=0$ for $n=0,\ldots 9]$.

The CVE algorithm can be summarized in the following three-step procedure:

- *Decomposition:* compute the wavelet coefficients $\tilde{\omega}_\lambda$ using the fast wavelet transform.[7]
- *Thresholding:* apply the thresholding function ρ_ε to the wavelet coefficients $\tilde{\omega}_\lambda$, thus discarding the coefficients with absolute values smaller than the threshold ε.
- *Reconstruction:* reconstruct the coherent vorticity field ω_C from the thresholded wavelet coefficients using the fast inverse wavelet transform.

The incoherent vorticity field is obtained by simple subtraction, i.e., $\omega_I=\omega-\omega_C$.

The thresholding function is given by

$$\rho_\varepsilon(a)=\begin{cases} a & \text{if } |a|>\varepsilon \\ 0 & \text{if } |a|\leqslant\varepsilon \end{cases}, \tag{8}$$

where ε denotes the threshold,

$$\varepsilon=\sqrt{4Z\ln N}, \tag{9}$$

where $Z=\frac{1}{2}\langle\omega,\omega\rangle$ is the enstrophy (which corresponds to half of the variance of the vorticity fluctuations) and N is the resolution. This threshold value allows for optimal denoising in a min-max sense, assuming the noise to be additive, Gaussian, and white.[8]

In summary, this decomposition yields $\omega=\omega_C+\omega_I$. Due to orthogonality, we have $\langle\omega_C,\omega_I\rangle=0$ and hence it follows that enstrophy is conserved, i.e., $Z=Z_C+Z_I$. Let us mention that the computational cost of the fast wavelet transform (FWT) is of $O(N)$.[7]

B. Compression rates

The results of the extraction are displayed in Table I. The compression rate is in both cases very significant: for the quasi-hydrodynamic case, 1.3% of the modes retain more than 99.9% of the energy and 97% of the enstrophy. For the quasi-adiabatic case, 1.8% of the modes retain 99.0% of the energy and 93% of the enstrophy. The contribution of the coherent vorticity to the radial flux is also given in Table I. The coherent modes, which contain most of the energy and enstrophy, are responsible for 99% of the radial particle density flux Γ_r in the quasi-hydrodynamic case, and for 98% of Γ_r in the quasi-adiabatic case. In other words, Γ_r is almost exclusively carried by the coherent structures.

C. Wavenumber spectra and probability density functions

Spectra and probability density functions (PDF), averaged over 512 realizations during the time interval $100<t\leqslant 612$, are shown in Fig. 2 for the total, coherent, and incoherent vorticity. The PDF of the total and coherent quasi-hydrodynamic vorticity is far from Gaussian and slightly skewed, while the quasi-adiabatic vorticity is much closer to Gaussianity. In both cases, the variance of the incoherent part is much smaller than the variance of the coherent part, which has the same PDF as the total. For the quasi-hydrodynamic case, the coherent part retains 97% of the variance of the vorticity fluctuations and therefore also 97% of the total enstrophy Z, with $Z=1.4$. For the quasi-adiabatic case, the coherent part retains 93% of the variance of the vorticity fluctuations and hence 93% Z, with $Z=3.4$. A similar result is observed in the enstrophy spectrum computed from the Fourier transform of the vorticity field, averaged over wavenumber shells of radius $|\boldsymbol{k}|$, the wavenumber. The total and coherent enstrophy are the same all over the inertial range, and at the highest wavenumbers, in the dissipation range, the incoherent part contributes to the spectral enstrophy density. Both coherent and incoherent contributions are spread all over the spectral range, but they present different spectral slopes in the inertial range and therefore different spatial correlations. From the integral wavenumber to the dissipation wavenumber, a negative slope for the coherent contribution, corresponding to long-range spatial correlations, is observed. The incoherent part shows a positive slope with a power-law dependence close to k^3 in the inertial range. This corresponds to an equipartition of kinetic energy in two dimensions. A similar result was obtained in three-dimensional isotropic Navier–Stokes turbulence.[8]

D. Scatter plots

We show in Fig. 3 scatter plots of the vorticity versus the electrostatic potential corresponding to the fields in Fig. 1. Both the total part and the incoherent part are shown. Since the coherent part is almost identical to the total part, it has been omitted. Also shown, superposed on the same figures, is the scatter plot corresponding to the zoom on the dipolar structures indicated by a white frame in Fig. 1. In the freely decaying hydrodynamic case, $c=0$, Joyce and Montgomery[19] showed that a functional relation $\phi(\omega)=\alpha\sinh(\beta\omega)$ should be expected, corresponding to a final state of decay depleted from nonlinearity. The parameters α and β are Lagrangian multipliers, necessary for maximizing the entropy under constraints. The value $1/\beta$ can be associated with a (negative) temperature.[19] Depletion from nonlinearity corresponds to steady solutions of the Euler equation, $[\omega,\phi]=0$, implied by the existence of a functional relation $\phi(\omega)$. Indeed drift-wave turbulence contains an internal instability which prevents the flow from decaying. This forcing is present in both cases considered here and a *sinh-Poisson* relation cannot be expected *a priori* for the global flows. Moreover, the two-field

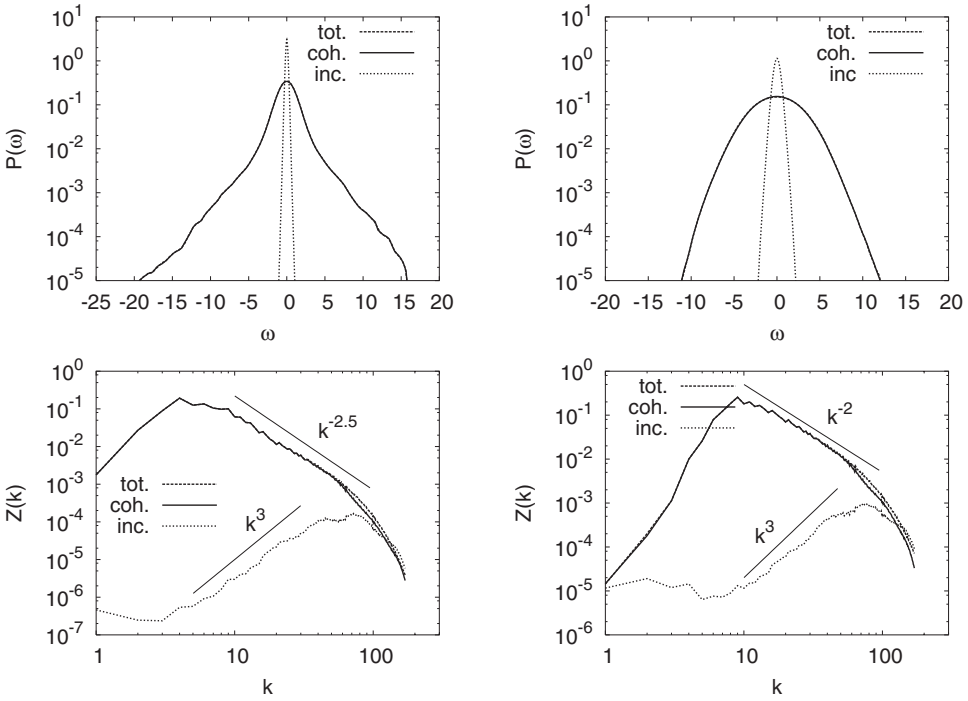

FIG. 2. Top: PDF of the vorticity. Bottom: Fourier spectrum of the enstrophy versus wavenumber. Left: quasi-hydrodynamic case. Right: quasi-adiabatic case. Dashed line: total field, solid line: coherent part, dotted line: incoherent part. Note that the coherent contribution (solid) superposes the total field (dashed), which is thus hidden under the solid line in all four figures. The straight lines indicating power laws are plotted for reference.

model [Eqs. (1) and (2)] contains two nonlinearities, first the polarization-drift nonlinearity in the vorticity equation, second the $E\times B$ nonlinearity in the density equation. The latter disappears in the adiabatic limit as n and ϕ are in phase, which corresponds to a linear functional relationship. In Fig. 3, a local depletion of the polarization-drift nonlinearity is seen for the quasi-hydrodynamic case. The scatter plot of $\phi-\omega$, corresponding to the dipolar structure, that is indicated by a white frame in figure 1 (left), is close to a *sinh-Poisson* relation (solid black curve) in spite of the presence of the forcing term. In the quasi-adiabatic case, the dipolar structure, which is indicated by a white frame in Fig. 1 (right), does not exhibit such a functional relation. In the incoherent parts (Fig. 3, bottom), no functional relation can be distinguished, which confirms that the incoherent part does not contain any structure, for both the quasi-hydrodynamic and quasi-adiabatic cases.

E. Strain versus vorticity

A question is now how to quantitatively distinguish between the structures in both cases. Intuitively it can be inferred that different regions of high vorticity in the quasi-adiabatic case involve strong mutual shearing, which

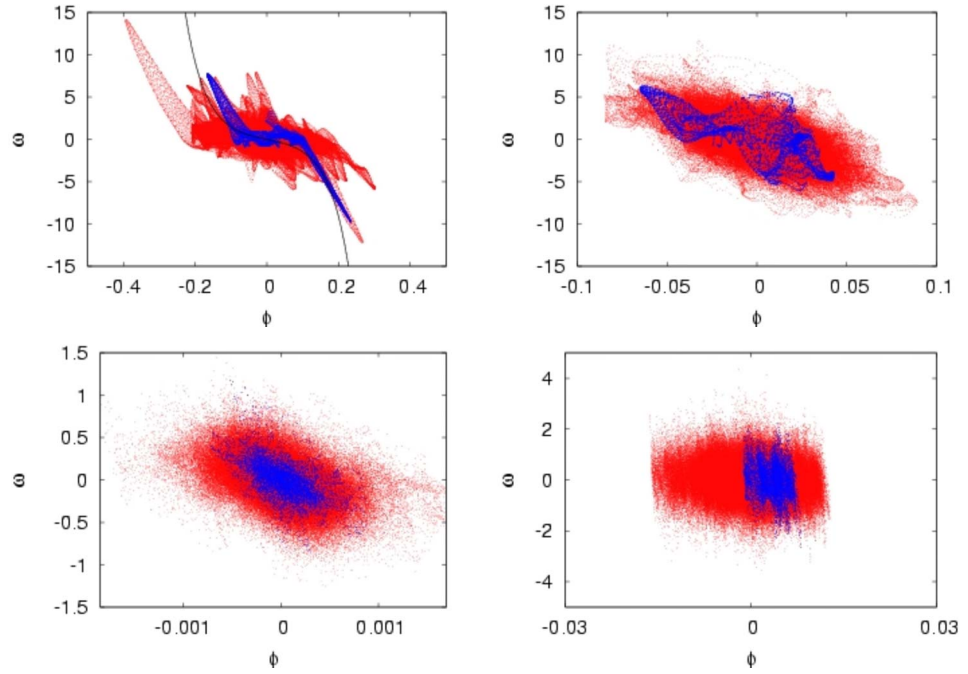

FIG. 3. (Color online) Scatter plot of vorticity against electrostatic potential for the coherent part (top) and incoherent part (bottom). Left, quasi-hydrodynamic case; right, quasi-adiabatic case. The light gray (red online) dots correspond to the total field, the dark gray (blue online) dots to the dipoles we have selected in Fig. 1.

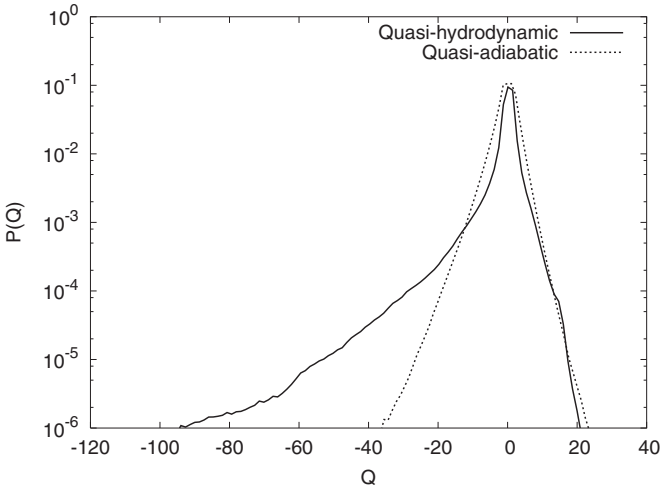

FIG. 4. PDF of the Weiss field Q for the quasi-hydrodynamic and quasi-adiabatic velocity fields.

strongly limits their lifetime and the chance to reach a functional relation $\phi(\omega)$. Koniges *et al.*[3] determined the lifetime of individual eddies compared to the eddy-turnover time τ_{over}, i.e., the time it takes for a fluid element in an eddy to make a 2π rotation. They estimated the lifetime of the quasi-hydrodynamic eddies to be approximately 10 τ_{over}, and the lifetime of the adiabatic eddies (for $c=2.0$) approximately τ_{over}. As mentioned in their paper, this measure is quite subjective and very time-consuming, especially if a full PDF of the lifetimes is to be obtained. Here we propose a simpler way to distinguish the coherent structures for the different regimes.

In fluid turbulence, the Weiss criterion Q (Ref. 20) is a local measure of the strain compared to the vorticity for a 2D velocity field. The Weiss field is defined as

$$Q = \tfrac{1}{4}(\sigma^2 - \omega^2), \tag{10}$$

with

$$\sigma^2 = \left(\frac{\partial u}{\partial x} - \frac{\partial v}{\partial y}\right)^2 + \left(\frac{\partial u}{\partial y} + \frac{\partial v}{\partial x}\right)^2. \tag{11}$$

u and v are two orthogonal components of the velocity vector. The Weiss criterion was proposed to identify coherent structures, but it may lead to ambiguous results because the underlying assumption that the velocity gradient varies slowly with respect to the vorticity gradient is not generally valid.[21] We apply the same criterion here to drift-wave turbulence[22–24] but not to identify coherent structures (this being done by the CVE method), but to distinguish between the quasi-hydrodynamic and quasi-adiabatic cases.

The PDF of the Weiss field (Fig. 4) reveals that it is its skewness that differentiates best the two fields. Indeed, it is more skewed toward negative Q for the quasi-hydrodynamic case than for the quasi-adiabatic case: the skewness is -11 for the former, compared to -2 for the latter. The PDF shows thus that in the quasi-hydrodynamic case, the probability to find rotationally dominated regions is larger, and the rotation exhibits much larger values, than in the quasi-adiabatic case. The variance of Q is comparable for the two cases (5 and 4 for the quasi-hydrodynamic case and the quasi-adiabatic case, respectively). The skewness of the Weiss field Q appears to be a good quantitative measure to distinguish between the two cases studied in the present work. In further studies, it can be investigated whether this measure can be used to identify coherence in different types of turbulent flows.

III. CONCLUSION AND PERSPECTIVES

In conclusion, we have applied the *coherent vortex extraction* method to dissipative drift-wave turbulence. The results show that we can identify the essential degrees of freedom (less than 2%) responsible for the nonlinear dynamics and transport. The coherent modes contain almost all the energy and enstrophy and contribute to more than 98% of the radial flux.

Evaluating the scatter plot of the vorticity versus the electrostatic potential, it is shown that the coherent structures in the quasi-hydrodynamic case are close to a state of local depletion of polarization-drift nonlinearity. In contrast, this is not the case for the quasi-adiabatic regime, where nonlinearity remains active and no *sinh*-functional relation between vorticity and electrostatic potential is observed. This depletion of nonlinearity in the quasi-hydrodynamic regime may explain the failure of the quasilinear estimate of the radial flux.[3] The skewness of the Weiss field yields a quantitative measure for the difference in nonlinear behavior of the coherent structures between the quasi-hydrodynamic and quasi-adiabatic cases.

The wavelet transform, or the proper orthogonal decomposition (POD), may become very useful to denoise particle-in-cell simulations of plasma turbulence.[25] A comparison of the performance of the POD and CVE method is currently being undertaken and will be reported in a future paper.

ACKNOWLEDGMENTS

Lionel Larchevêque is acknowledged for supplying and helping with a routine to compute the Weiss field. Wendel Horton is acknowledged for comments on the manuscript. One of us (S.F.) is grateful to the French Ministry of Foreigh Affairs for the fellowship "Bourse du Gouvernement Français."

This work was supported by the *Agence Nationale de la Recherche* under the contract *Méthodes Multi-échelles pour l'analyse et la simulation numérique en Turbulence Fluide et Plasma* (M2TFP).

[1] X. Garbet, C. R. Phys. **7**, 573 (2006).
[2] S. J. Zweben, Phys. Fluids **28**, 974 (1985).
[3] A. E. Koniges, J. A. Crotinger, and P. H. Diamond, Phys. Fluids B **4**, 2785 (1992).
[4] T. Dudok de Wit, S. Benkadda, P. Gabbai, and A. D. Verga, Phys. Rev. E **52**, 6753 (1995).
[5] W. Horton and Y. H. Ichikawa, *Chaos and Structures in Nonlinear Plasmas* (World Scientific, Singapore, 1996).
[6] G. Hu, J. A. Krommes, and J. C. Bowman, Phys. Plasmas **4**, 2116 (1997).
[7] M. Farge, Annu. Rev. Fluid Mech. **24**, 395 (1992).
[8] M. Farge, G. Pellegrino, and K. Schneider, Phys. Rev. Lett. **87**, 054501 (2001).

[9]M. Farge, K. Schneider, and P. Devynck, Phys. Plasmas **13**, 042304 (2006).
[10]B. Scott, New J. Phys. **4**, 52 (2002).
[11]A. Hasegawa and M. Wakatani, Phys. Rev. Lett. **50**, 682 (1983).
[12]M. Wakatani and A. Hasegawa, Phys. Fluids **27**, 611 (1984).
[13]W. Horton, Phys. Rep. **192**, 1 (1990).
[14]A. Hasegawa and K. Mima, Phys. Fluids **21**, 87 (1977).
[15]W. Horton, Rev. Mod. Phys. **71**, 735 (1999).
[16]A. Arakawa, J. Comput. Phys. **1**, 119 (1966).
[17]S. Mallat, *A Wavelet Tour of Signal Processing* (Academic, New York, 1998).
[18]M. Farge, K. Schneider, and N. Kevlahan, Phys. Fluids **11**, 2187 (1999).
[19]G. Joyce and D. Montgomery, J. Plasma Phys. **10**, 107 (1973).
[20]J. Weiss, Physica D **48**, 273 (1991).
[21]C. Basdevant and T. Philipovitch, Physica D **73**, 17 (1994).
[22]T. S. Pedersen, P. Michelsen, and J. J. Rasmussen, Phys. Plasmas **3**, 2939 (1996).
[23]S. V. Annibaldi, G. Manfredi, and R. O. Dendy, Phys. Plasmas **9**, 791 (2002).
[24]V. Naulin and K. H. Spatschek, Phys. Rev. E **55**, 5883 (1997).
[25]S. Gassama, E. Sonnendrücker, K. Schneider, M. Farge, and M. Domingues, ESAIM Proceedings (EDP Sciences, 2007), Vol. 16, p. 195.